

1G Shaking Table Tests on Saturated Fill Slope Focusing on Resonance Phenomena

Tests sur table à secousses 1G de pentes de talus artificiels saturés avec concentration sur les phénomènes de résonance

Hidehiko Murao & Kentaro Nakai

Department of Civil Engineering, Nagoya University, Japan, murao.hidehiko@h.mbox.nagoya-u.ac.jp

ABSTRACT: With the aim of determining the mechanisms of deformation on fill slopes at the time of an earthquake, 1G shaking table tests were carried out on a saturated model slope focusing on the frequency properties. From the results, it was found that the stability of fill slopes in an earthquake is determined not only by the magnitude of the input acceleration but also strongly depends on the relationship between the natural frequency of the constructed embankment slope and the input frequency. Specifically, the following were concluded. When the input frequency is substantially equal to the initial natural frequency of the slope surface, resonance is produced from the initial stage, and the acceleration is amplified (increase in inertial force). Simultaneous to accumulation of plastic deformation, the mean effective stress is reduced and stiffness decreases. Eventually, the stiffness is lost locally in a shallow part where the confining pressure is small, and slip occurs locally. As the excitation stage increases, the slip extends and expands, and slip occurs in deeper parts.

RÉSUMÉ : Dans le but de déterminer les mécanismes de déformation des pentes de talus artificiels lors d'un tremblement de terre, des tests sur table à secousses 1G ont été effectués sur une maquette de pente saturée, en se concentrant sur les propriétés des fréquences. D'après les résultats, on constate que la stabilité des pentes de talus artificiels lors d'un séisme n'est pas seulement déterminée par la magnitude de l'accélération en entrée, et qu'elle dépend également fortement de la relation entre la fréquence naturelle du talus artificiel et la fréquence en entrée. En particulier, nous avons conclu ce qui suit. Quand la fréquence d'entrée est sensiblement égale à la fréquence naturelle initiale de la surface de la pente, la résonance se produit dès l'étape initiale, et l'accélération est amplifiée (augmentation de la force d'inertie). Simultanément à l'accumulation de la déformation plastique, la contrainte effective moyenne est réduite et la rigidité diminue. Tôt ou tard, la rigidité est perdue localement sur une zone peu profonde où la pression de confinement est faible, et un glissement localisé se produit. À mesure que la phase d'excitation augmente, le glissement s'étend et s'accroît, et le glissement se produit sur des parties plus profondes.

KEYWORDS: Shaking table test, Slope stability, Failure

1 INTRODUCTION

About 73% of the national land of Japan is mountainous, and flat terrain is limited. Therefore, the method of cutting the hilly part of a hilly area and using the soil generated to form an embankments in a nearby valley or low-lying area has been widely used. The slopes constructed by this method are found in linear structures such as roads and railways, as well as in residential areas on the outskirts of cities, and have contributed to urban expansion. On the other hand, in the 2007 Noto Peninsula Earthquake, it was reported that a large-scale landslide occurred on a fill slope on a high quality and sufficiently compacted toll road (Tameshige et al., 2009). Also, in the 2011 Off the Pacific Coast of Tohoku Earthquake, even on fill slopes in which landslide countermeasures had been implemented at the same time (pile works and groundwater drainage works), it was reported that although there were locations where the countermeasures were effective, landslides nonetheless occurred nearby (Murao et al., 2013). From these examples, it can be concluded that the current design methods and countermeasures rely greatly on experience and that they are not sufficient to prevent damage. The damage to fill slopes due to major earthquakes is large, so there is a demand for seismic evaluation methods and countermeasures that can correctly evaluate the occurrence of damage and reflect the deformation mechanisms. To date, lots of researches have been carried out. However, many aspects of the deformation mechanisms of complex fill slopes are still unclear.

This paper presents the results of 1G shaking table tests carried out to investigate the change in acceleration amplification factor and pore water pressure behavior occurring in the interior of embankments, focusing on the resonance of fill

slopes, in other words, the relationship between the natural frequency and the input frequency, and discusses the deformation mechanisms of saturated fill slopes during an earthquake.

2 PREPARATION OF THE MODEL SLOPE

A model slope envisaged to be a 1/50 scale model of a fill slope consisting of a bedrock part and an embankment part was constructed within a stainless steel soil tank, and it is considered that a plane strain condition can be obtained. As shown in Fig. 1, 7 accelerometers (ch. 1 to 6 and 8) and 7 pore water pressure meters (ch. 9 to 15) were embedded in the embankment while it was being constructed, and 1 accelerometer (ch. 7) was installed on the bottom of the soil tank to measure the input excitation.

The bedrock material was Mikawa silica sand (Nos. 4, 5, 56, 6, and 7) mixed in the proportions 1:1:1:1 by mass, to which a cementitious stabilizer was added at the rate 150 kg/m³. The bedrock material was compacted with a water content $w = 15\%$, and after curing for 28 days, it was formed into a stair shape. The reason why soil-cement was used as the bedrock material is that the bedrock of constructed embankment slopes that have deformed in an earthquake have frequently been Tertiary or Pleistocene rocks and relatively harder than the embankment part, so the aim was to reproduce conditions in which the strength difference between the embankment part and the bedrock part was large. Also, by increasing the resistance between the bedrock part and the embankment part by forming the boundary in a stair shape, the occurrence of slip at the boundary was prevented. Table 1 shows the physical properties for the embankment material. The embankment material was

formed by mixing Mikawa silica sand (Nos. 4, 5, 6, and 7), DL clay, and blue clay in the proportions 3:3:3:3:4:4 by mass. This was because the embankment material of the fill slopes that damaged in earthquakes in many cases was soil arising from cutting nearby hills and was intermediate soil that included fine particles. The density of the embankment part was controlled to adjust it so that the water content $w = 12\%$, the dry density $\rho_d = 1.72 \text{ g/cm}^3$, and the degree of compaction $D_c = 90\%$. Compaction was carried out in 15 layers (1 layer = 2 cm) to achieve horizontal stratification. Then the seepage surface was raised to the ground surface in stages over a period of 30 hours, maintaining the horizontal stratification. After leaving the model slope in the fully submerged state for 10 hours, the embankment was excavated and formed into a specific slope shape. The reason for allowing seepage until the model slope could be regarded as saturated state was because fill slopes are supplied with groundwater from the slopes to the rear, so the groundwater level is frequently formed close to the ground surface. Note that when allowing the water to seep into the model slope, the hydrostatic pressure due to the rise in pore water pressure was checked, and there was no change after forming the slope, so the model slope was considered to be in the saturated state.

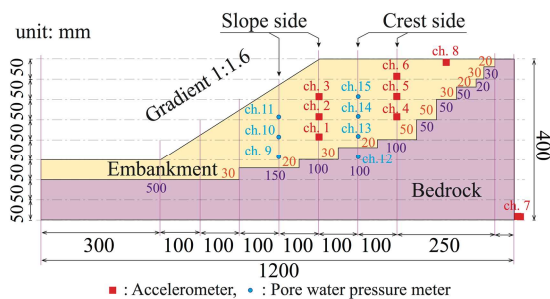


Figure 1 Outline of the model slope

Table 1. Physical properties for the embankment material

Soil particle density ρ_d (g/cm ³)	2.698
Clay fraction (%)	14.7
Silt fraction (%)	28.2
Fine fraction (%)	32.3
Medium sand (%)	16.7
Coarse sand (%)	8.1

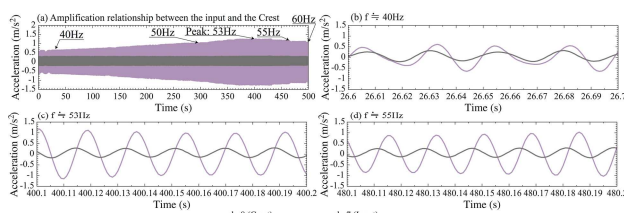


Figure 2 Result of the sweep test (relationship between input and measured acceleration amplitude)

3 NATURAL FREQUENCY OF THE MODEL SLOPE

In order to carry out the study focusing on resonance phenomena, a sweep test was carried out to determine the natural frequency of the model slope. The sweep frequency was a sine wave with a constant acceleration amplitude of 0.2 m/s^2 , the frequency was increased from 10 to 60 Hz, and the acceleration amplitude was measured with an accelerometer (ch. 8) installed on the crown of the embankment. Fig. 2 shows the input acceleration (ch.7) and the acceleration measured at the crown. The measured acceleration of the crown increases as the input frequency is changed up to around 390 s, and thereafter it is considered to be attenuated, so it can be seen that the input

frequency at the time at which the amplitude is greatest is the natural frequency of the model slope. From the result, it can be seen that the natural frequency of the model slope is around 50 Hz, so in the below 1G shaking table tests, 50 Hz excitation was adopted as the input frequency close to the natural frequency.

4 TEST RESULTS AND DISCUSSION

The input acceleration was a sine wave with a constant frequency (50Hz), and excitation was carried out in stages, increasing the excitation in steps of 0.5 m/s^2 , from 0.2 to 5.2 m/s^2 . The excitation duration of each stage was 60 seconds. An interval of 240 seconds was provided between stages to prepare for the next excitation. The data from the accelerometers and pore water pressure meters were acquired by sampling at a frequency of 1,000 Hz. Fig. 3 shows the measured acceleration and corresponding change in amplification factor. Fig. 4 shows the change in excess pore water pressure ratio. Although the measurement was conducted in both slope and crest side, the results showed similar tendency in both side. Therefore, measurement results at crest side are omitted here. Photograph 1 shows a side view of the model prior to excitation and at stage 11 (input acceleration of 5.2 m/s^2). The 2 slip surfaces within Photograph 1 were determined from the displacements of the markers installed on the side surface and from the change in amplification factor and the pore water pressure behavior as described later.

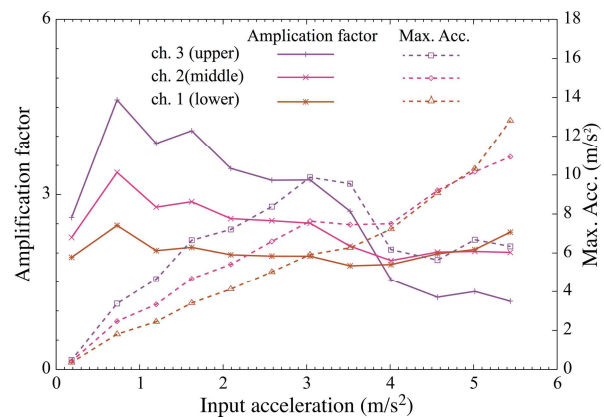


Figure 3 The measured acceleration and corresponding change in amplification factor

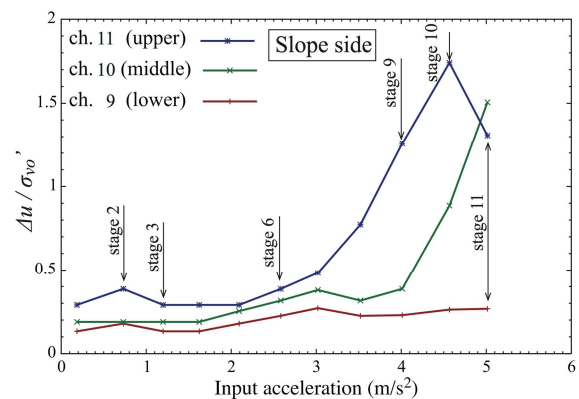
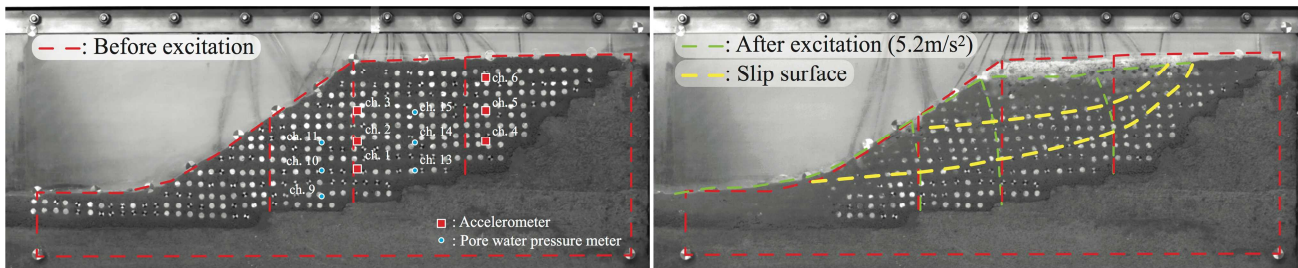


Figure 3 The change in excess pore water pressure

Stage 1 to 2 “process of resonance”

Comparing the amplification factors in the depth direction from Fig. 3, it can be seen that in the initial stage, the amplification is larger at positions close to the ground surface, with the following relationship.

$$\text{ch. 1 (lower)} < \text{ch. 2 (middle)} < \text{ch. 3 (upper)}$$



Photograph 1 Side view of the model prior to excitation and at step 11 (input acceleration of 5.2 m/s²).

The maximum amplification factor is observed in stage 2 (input acceleration of 0.7 m/s²). This is because the input frequency is close to the natural frequency of the model slope, so resonance occurs. Moreover, the oscillations become larger in the shallower parts compared with the deeper parts. Resonance is produced at this stage, so even though the input acceleration is small, large oscillations are produced in the embankment part.

Stage 3 to 8 “process of reduction of the natural frequency”

As the input acceleration is further increased (stages 3 to 8), the relationship of the magnitude of the amplification factor in the depth direction is maintained as the acceleration increases at each measurement point, but the amplification factor in the shallow to middle parts of the embankment is reduced. The reason why the amplification factor reduces from stage 3 (input acceleration of 1.2 m/s²) onwards is considered to be elimination of the resonance with the accumulation of small plastic deformations associated with excitation. In other words, from the viewpoint of elasto-plasticity, the following can be considered.

1. At the beginning of this stage, the input excitation was still small, but the amplification factor was still 3 or higher, so plastic deformation gradually accumulated on the model slope. The stress ratio during oscillation is not large enough to reach the critical state (failure), so the plastic deformation acts as plastic compression.
2. The drainage condition during the test can be considered as undrained (no volumetric change), so elastic expansion is produced as a result of the plastic compression. Therefore, the mean effective stress is reduced, and the pore water pressure increases.
3. Stiffness is reduced as the mean effective stress is reduced, so the natural frequency of the model slope as a system reduces. Although no clear deformation can be seen in the model slope, water was discharged at the ground surface from excitation stage 3 onwards. The reduction in the amplification factor from stage 3 onwards is greater in the shallower parts, so it is considered that the closer to the surface of the slope, where the confining pressure is smaller, the greater the accumulation of plastic deformation. This means that the discharge of water is the result of seepage accompanied with the increase in pore water pressure within the model slope as described above. No increase in the values of the pore water pressure meters can be seen even in the pore water pressure meter in the shallowest part, but it is considered that the pore water pressure increased in the much shallower parts than the place where pore water pressure meters were embedded.

Stage 9 to 10 “process of formation of slip in the shallow part”

At stage 9 (input acceleration of 4.2 m/s²), an open crack was generated at the surface, and a flow slip in the shallow part is clearly seen. At this stage, there is a significant reduction of the amplification factor (ch. 3) in the shallow part of the slope, and the relationship of the magnitude of the amplification factor in the depth direction is reversed, as follows.

$$\text{ch. 3 (upper)} < \text{ch. 1 (lower)} < \text{ch. 2 (middle)}$$

Figure 5 shows the excess pore water pressure ratio and the acceleration wave form under stage 9 of excitation (input acceleration of 4.2 m/s²). In the final stage of excitation, the

excess pore water pressure ratio at the surface (ch. 11) increases gradually during excitation and acceleration (ch. 3) is gradually attenuated after reaching a peak of 10 m/s². The generation of slip and reversal of the relationship of the magnitude of the amplification factor can be considered as follows.

1. As a result of the increase in input acceleration, plastic deformation spreads further, and the mean effective stress is reduced.
2. The reduction in mean effective stress increases as depth decreased, and the confining pressure is smaller in the shallower parts, so the excess pore water pressure ratio exceeds 1.0.
3. Stiffness is further reduced locally, and as a result of repeated loading, the soil is disturbed and the strength is reduced.
4. The acceleration around the position where slip is occurring is attenuated by internal dissipation, so the amplification factor is reversed.

In other words, at the top of the embankment, large oscillations are experienced as inertial forces increase. Stiffness and strength are reduced as plastic deformation accumulates, and at this stage, it is considered that slip was generated.

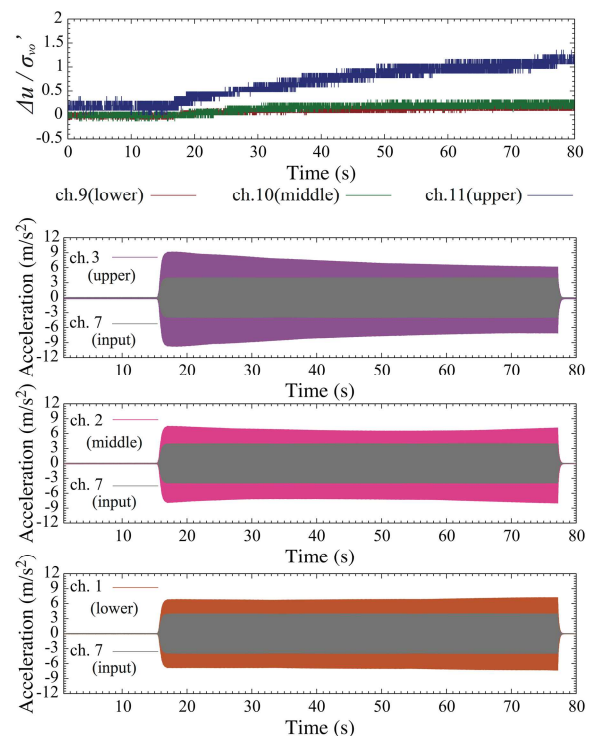


Figure 5 Excess pore water pressure ratio and acceleration wave form under stage 9 of excitation (input acceleration of 4.2 m/s²)

Stage 11 onwards “process of occurrence of slip in the deep parts”

In stage 11 (input acceleration of 5.2 m/s²), a deep slip occurred from the crown of the embankment toward the toe of the slope. At this stage, the amplification factor in the middle of the slope

(ch. 2) is significantly reduced, and the relationship of the magnitude in the depth direction is reversed, as follows.

ch. 3 (upper) < ch. 2 (middle) < ch. 1 (lower)

Figure 6 shows the excess pore water pressure ratio and the acceleration wave form on the slope surface side in the case of excitation stage 11 (input acceleration of 5.2 m/s²). As in the shallow parts in excitation stage 9, as described previously, the excess pore water pressure ratio exceeds 1.0 in the middle of the slope surface (ch. 10), and the acceleration in the middle (ch. 2) is gradually attenuated after reaching a peak of 7.5 m/s². Separately from the flow slip close to the surface that occurred in stage 9, a slip was generated in the deep part in stage 11. It is considered that this slip occurred by the same mechanism as for the shallow part, namely reduction in stiffness and strength associated with the accumulation of plastic deformation with the increase in inertial forces (in the soil mass above the slip surface that occurred) and the repeated loading process including resonance.

The excess pore water pressure ratio at the shallow part (ch. 11), which tended to rise until this stage, began to reduce after 50 seconds and ultimately became negative (occurrence of negative pore water pressure). This occurrence of negative pressure is considered to be due to the occurrence of a positive dilatancy effect near the slip surface caused by the large plastic deformation that occurred at the slip of the shallow part of the embankment in stage 9, resulting in local recovery of stiffness. Moreover, the acceleration associated with the recovery of stiffness reversed the amplification. Although the results are omitted here, we have confirmed that embankment material exhibits positive dilatancy properties by triaxial compression test when a large shear deformation is imposed.

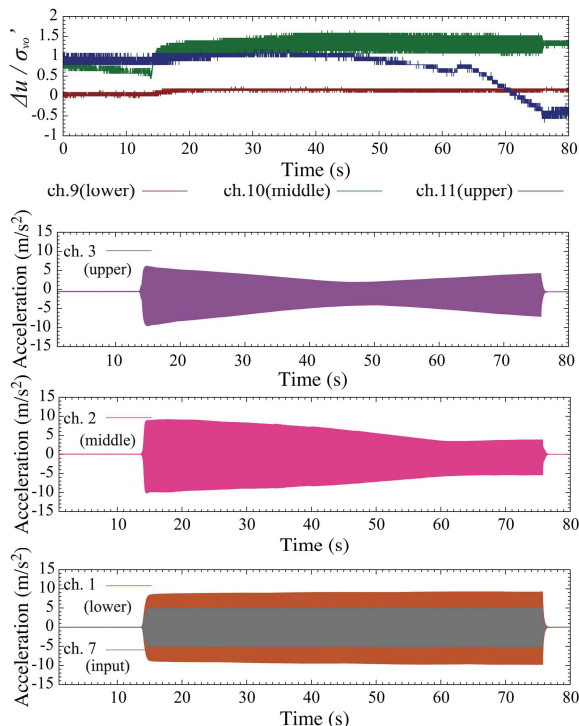


Figure 6 Excess pore water pressure ratio and acceleration wave form under stage 11 of excitation (input acceleration of 5.2 m/s²)

Summarizing the above, when the input frequency is virtually the same as the natural frequency, resonance occurs from the initial stage of excitation, and the acceleration is amplified. As plastic deformation is accumulated, the mean effective stress is reduced. Eventually, stiffness and strength are reduced locally at the shallow part of the embankment where the confining pressure is small. At the same time, even though

the amplification factor is reduced, the magnitude of the acceleration at the shallow part has already increased, so the inertial forces increase, and a slip was generated at the shallow part. In addition, as the input acceleration increases, slip was progressively generated in the deeper part by the same mechanism.

6 CONCLUSIONS

The objective of this paper was to clarify the deformation mechanisms of fill slopes during earthquakes, and as part of this, 1G shaking table tests were carried out on saturated model slopes modeling a typical fill slope, focusing on the frequency properties. First, a sweep test was carried out with a sine wave of constant acceleration amplitude (0.2 m/s²), from which it was determined that the natural frequency of the model slope considered to be the lowest prior to excitation was 50 Hz. Then 1G shaking table tests were carried out with the input frequency of 50 Hz. Excitation was carried out by applying a sine wave with a constant frequency, and the acceleration amplitude was increased in stages. The main findings are as follows.

1. Where the input frequency was almost equal to the initial natural frequency of the slope surface, resonance occurred from the initial stages of excitation, the acceleration of the slope surface was amplified, and the inertial forces increased.
2. Simultaneous to accumulation of plastic deformation, the mean effective stress was reduced, stiffness and strength were eventually reduced locally at the shallow part of the embankment, where the confining pressure was low (excess pore water pressure ratio exceeded 1.0), and a slip was generated in the shallow part. The discharge of water from the surface was evidence of the reduction in mean effective stress.
3. As the acceleration further increased, even though the acceleration reduced in the shallow part, the acceleration and inertial forces increased below the slip line, so the mean effective stress reduced, and a slip occurred in the deep part.

We have also conducted the 1G shaking table tests with different input frequencies. We cannot show the details because of space restrictions, but we found the following result.

4. Evaluation of the seismic stability of fill slopes depends not only on the magnitude of the acceleration of the input seismic wave but is also strongly dependent on the relationship between the natural frequency of the constructed embankment slope and the input frequency.

ACKNOWLEDGEMENTS

The authors wish to acknowledge Prof. Toshihiro Noda of Nagoya University for his apposite guidance and informative discussions of this research. This work was supported by JSPS KAKENHI Grant Number JP25249064.

REFERENCE

- Murao, H., Kamai, T. and Ohta, H. 2013, Slope disaster in urban residential region by earthquake - Take "the 2011 off the pacific coast of Tohoku earthquake" as an example -, *Journal of the Japan Society of Engineering Geology*, 53(6), 292-301. (in Japanese)
- Tameshige, M., Kawamura, K., Komada, S., Miyamura, M., Haibara, T. and Mouri, T. 2009, Noto peninsula earthquake damage to Noto toll road and its restoration - Embankment damage and countermeasure work -, *Japanese Geotechnical Journal* 4(4), 289 - 305. (in Japanese)